Supporting Information

Nanosecond laser photothermal effect-triggered amplification of photochromic reaction in diarylethene nanoparticles

Y. Ishibashi,[a] S. Nakai,[a] K. Masuda,[a] D. Kitagawa,[b] S. Kobatake,[b] and T. Asahi*[a]

[a.]Department of Materials Science and Biotechnology, Graduate School of Science and Engineering,

Ehime University, Matsuyama, Ehime, 790-8577, Japan

E-mail: asahi.tsuyoshi.mh@ehime-u.ac.jp

[b.]Department of Applied Chemistry, Graduate School of Engineering,

Osaka City University, Sumiyoshi, Osaka 558-8585, Japan

Contents

1. Sample preparation

Here, we describe the sample preparation and the photophysycal properties of **DE(c)-NP**.

[1,2-Bis(2-methoxy-5-phenyl-3-thienyl)perfluoro-cyclopentene] (**DE**) was synthesized and purified.[1] Ethanol (EtOH, spectral grade) was purchased from FUJIFILM Wako Pure Chemical Corporation and was used without further purification. Water was distilled and used. The room temperature was set to 20±1℃ in all the measurements. In this study, as a solid-phase sample, we chose **DE** nanoparticles (**DE-NPs**) dispersed in water, which allow us to use solution-phase techniques to study reversible solid-state photochemical reactions.

Aqueous **DE-NP** colloids were prepared by the conventional reprecipitation method.[2,3] First, a 3 mg of **DE(o)** (552.55 g mol^{-1}) was dissolved into 2 ml EtOH (2.7×10^{-3} M) with sonication for 10 min., and a 0.2 ml of the EtOH solution was injected into vigorously stirred water (10 ml) using a microsyringe, resulting in **DE(o)-NPs** colloids (5.3×10^{-5} M) with slight white turbidity. After aging time for 1 day in the dark room, the **DE(o)-NPs** irradiated at 330±5 nm light (11 mW cm^{-2}) evolved into the pale-blue colour due to the formation of **DE(c)**. After the photostationary state (PSS) was reached within a few minutes, the **DE(c)-NP** colloids were used for steady-state and time-resolved spectroscopic measurements. The size distribution of the sample **DE(c)-NP** was obtained by the dynamic light scattering (DLS) measurement (Malvern, ZETASIZER Nano-S), showing that the Z-average was 67 nm, and the PDI was 0.084. We confirmed that the **DE(c)-NPs** were stably dispersed in water for 1 week and they can repeatedly undergo the photochromic reactions (cyclization and cycloreversion reactions) more than 10 times under CW light irradiation without the photodegradation.

Next, to obtain the concentration ratio of **DE(c)** to **DE(o)** in **DE-NP** at PSS, the procedure was as follows. A 2 mL of the aqueous **DE-NP** colloids after reaching the PSS were dried under reduced pressure for a few days in the dark room, and the obtained blue solids were solved in EtOH (2 mL) with sonication for 10 min.. By measuring the absorption spectrum of this EtOH solution, we obtained the concentration of the **DE(c)** to be 3.7×10^{-5} M because the molar absorption coefficient of **DE(c)** in EtOH, ε_c^{EtOH} was known (e.g. 5000 $M^{-1}cm^{-1}$ at 532 nm, and 15000 $M^{-1}cm^{-1}$ at 630 nm). This indicated that the concentration ratio of **DE(c)** to **DE(o)** at PSS was 70%. The sample **DE-NP** in this study consist of a mixture of 70% **DE(c)** and 30% **DE(o)**. In this study, the **DE(c)**-rich

NP is abbreviated as **DE(c)-NP**. The molar absorption coefficient of the **DE(c)-NP**, ε_c^{NP} in the visible region was also obtained by using the above concentration and the steady-state absorption spectrum of **DE(c)-NP** as shown in Figure S1 (d). For example, ε_c^{NP} was 4400 $M^{-1}cm^{-1}$ at 532 nm, and 13100 $M^{-1}cm^{-1}$ at 630 nm.

On the other hand, **DE(c)** in EtOH solution as a reference was prepared with the same manner. A 0.2 ml of the EtOH solution with the concentration of 2.7×10^{-3} M was injected into another EtOH solution (10 ml) using the microsyringe, resulting in the colourless EtOH solution of **DE(o)** (5.3×10^{-5} M). When the solution was irradiated by 330±5 nm light (11 mW cm^{-2}) for a few minutes to reach the PSS, the colour of the solution changes to pale blue. At PSS, the concentration ratio of **DE(c)** to **DE(o)** in the EtOH solution was >99%, which was in good agreement with the reported value.[1] This **DE(c)** in EtOH was used as a reference sample.

Steady state-absorption spectra of the **DE** in EtOH and the **DE-NP** in water was measured with a JASCO V570 spectrophotometer. The results are shown in Figure S1(b) for the EtOH solution and (c) for the **DE-NP** colloids. In the EtOH solution, the **DE(o)** has the absorption band having two peaks at 270 nm and 310 nm in the UV region. Upon 330-nm CW-light irradiation for 5 min. to attain the PSS, the absorption band having a peak at 630 nm due to the **DE(c)** was observed in the visible region. On the other hand, in the **DE-NP**, the **DE(o)** also has the absorption band with two peaks at 270 nm and 310 nm in the UV region and the tail in the visible region due to the light scattering of the nanoparticles. Except for the tail, the spectral shape of **DE(o)** was consistent with that of the EtOH solution. After reaching the PSS, the absorption spectrum of **DE(c)-NP** in the visible region has a peak at 630 nm and clear shoulder at 700 nm and it was broader than that of the EtOH solution as shown in Figure S1(d). This shoulder will derive from mutual interactions between neighbouring **DE** molecules and limited molecular motions.

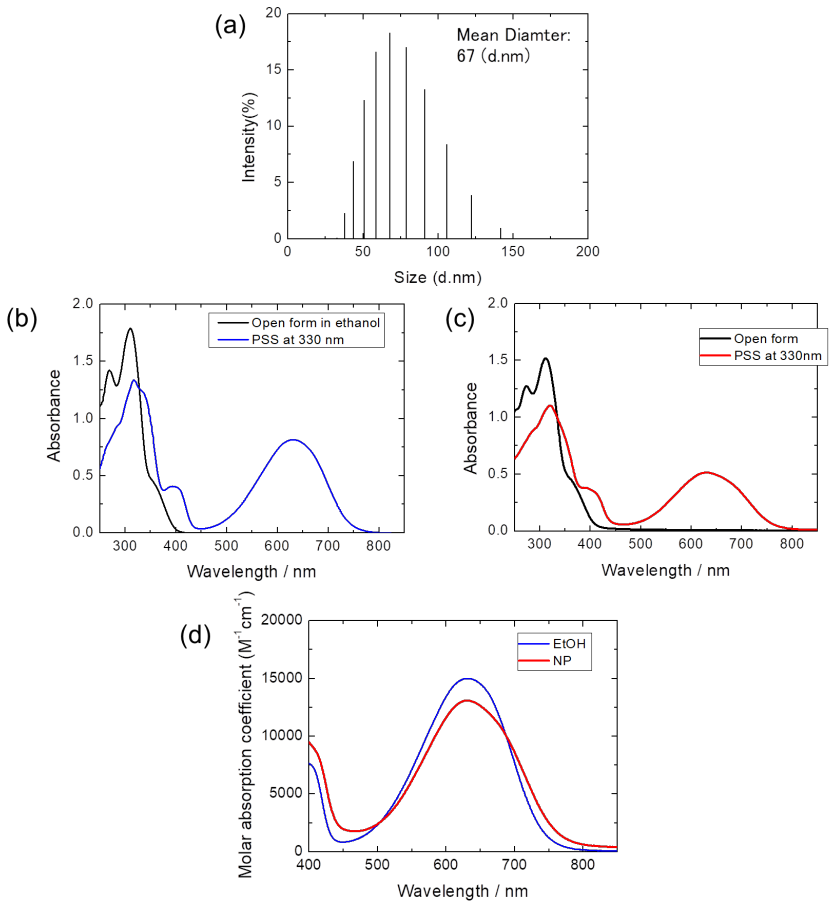

Figure S1. (a) Size distribution of aqueous **DE(c)-NP** colloids by DLS. (b) Steady-state absorption spectra of **DE** in EtOH. (c) Steady-state absorption spectra of aqueous **DE-NP** colloids. (d) Comparison of the molar absorption coefficient of the **DE(c)** EtOH solution and the **DE(c)-NP** in the visible region.

2. Estimation of cycloreversion reaction yield upon CW light irradiation

The experimental setup was similar to that for single-shot ns Nd^{3+}: YAG laser pulse exposure as shown in figure S3. A 300-W Xe lamp (MAX-301, Asahi Spectra) was used as a light source. Irradiated wavelength was tuned to be 550±20 nm (11 mW) by using a band-pass filter and a mirror module. A temperature-controllable sample cell unit (TLC50F, Quantum Northwest) was used. The quartz cell (1 cm × 1 cm × 3 cm) was used, and the sample volume was 2 mL. After confirming the temperature of the **DE(c)-NP** colloids by a thermocouple, the temporal evolution of the absorbance of **DE(c)-NP** at 630 nm upon visible CW-light irradiation was measured. During the measurement, the sample was stirred with a small magnetic stirrer (500 rpm). The obtained profile was analysed by applying eq. S1. This equation was derived for the spectral evolution via photochemical reaction under the CW-light irradiation, and the derivation was described in ref. 4 in detail.

$$ln\left(10^{A(t)}-1\right)-ln\left(10^{A(0)}-1\right)=-ln10\times\Phi_{CO}^{NP}\times\varepsilon_c^{NP}\times I\times t \qquad \text{(eq. S1)}$$

Here, $A(0)$ and $A(t)$ are the absorbance of **DE(c)-NP** at 630 nm before the CW-light irradiation, and at a time, t after the irradiation, respectively. Φ_{CO}^{NP} is the cycloreversion reaction quantum yield of the **DE(c)-NP**, ε_c^{NP} is the molar absorption coefficient of the **DE(c)-NP** at 550 nm, and I is the fluence of the CW-light.

Figure S2(a) shows time profiles of the absorbance of **DE(c)-NP** monitored at 630 nm, where the calculated value of $\ln(10^{A(t)}-1)-\ln(10^{A(0)}-1)$ is plotted as a function of the time, t. It was noted that the temperature of the **DE(c)-NP** colloids was set to 20℃. The linear relation between $\ln(10^{A(t)}-1)-\ln(10^{A(0)}-1)$ and t holds for the cycloreversion reaction of the **DE(c)-NP**, and the slope ($slope^{NP}=-ln10\times\Phi_{CO}^{NP}\times\varepsilon_c^{NP}\times I$) was calculated to be -1.55×10^{-4} with the linear fit. However, it is difficult to obtain the accurate value of I under the CW-light irradiation. To solve this problem, we calculated the value of I by obtaining the slope of the EtOH solution ($slope^{\mathrm{EtOH}}$) because the cycloreversion reaction quantum yield (Φ_{CO}^{EtOH}, 1.1×10^{-4}) and the molar absorption coefficient (ε_c^{EtOH}, 5000 $M^{-1}cm^{-1}$) of the **DE(c)** in EtOH are known.[1] It was noted that we tuned the same value of the 550-nm CW-light power (11±0.5 mW) in both measurements. So, Φ_{CO}^{NP} was obtained by using eq. S2.

$$\Phi_{CO}^{NP} = \frac{slope^{NP}}{slope^{EtOH}} \times \frac{\varepsilon_c^{EtOH}}{\varepsilon_c^{NP}} \times \Phi_{CO}^{EtOH} \qquad \text{(eq. S2)}$$

Time profile of the absorbance of the EtOH solution is also shown in Figure S2(a). The slope ($slope^{EtOH} = -ln10 \times \Phi_{CO}^{EtOH} \times \varepsilon_c^{EtOH} \times I$) was calculated to be -5.57×10^{-4} with the linear fit. The $slope^{NP}$ grew smaller than the $slope^{EtOH}$. Considering that the ε ratio of the EtOH (5000 $M^{-1}cm^{-1}$) to the NP (4400 $M^{-1}cm^{-1}$) was 1.18 and Φ_{CO}^{EtOH} was 1.1×10^{-4}, we estimated the cycloreversion reaction quantum yield of the **DE(c)-NP** to be 0.36×10^{-4} at 20℃.

Next, to obtain the activation energy for the cycloreversion reaction of **DE(c)-NP**, we examined the temperature dependence of time profiles of the absorbance at 630 nm upon 550-nm CW-light irradiation. The temperature-controllable sample cell unit was employed, and the temperature of the aqueous **DE(c)-NP** colloids was varied from 20℃ to 80℃. The quartz cell (1 cm × 1 cm × 3 cm) was used, and the sample volume was 2 mL. During the measurement, the sample was stirred with a small magnetic stirrer (500 rpm). We confirmed that the temperature of the sample was kept before and after the measurement and the heating did not induce aggregation and degradation of the **DE(c)-NPs**. The reaction quantum yield at each temperature was calculated with the above same manner. The yield of 0.36×10^{-4} at 20℃ was used as a reference and ε_c^{NP} at each temperature was also calculated from the absorption spectrum. Figure S2(b) shows the relation between $\ln(10^{A(t)}-1) - \ln(10^{A(0)}-1)$ and t. The linear relation at any temperature was observed. The slope increased with an increase in the temperature from 20℃ to 80℃. By comparing the slope at each temperature with that at 20℃, the cycloreversion reaction yield was calculated. Figure S2(c) shows the temperature dependence of the cycloreversion reaction yield of **DE(c)-NP**. The Y-axis presents $ln(\Phi_{CO}^{NP})$ and the X-axis is the inverse of the temperature of the colloids (1000/T). The Φ_{CO}^{NP} increased with increasing in the temperature. From the linear fit, the activation energy was calculated to be 23 kJ mol^{-1}.

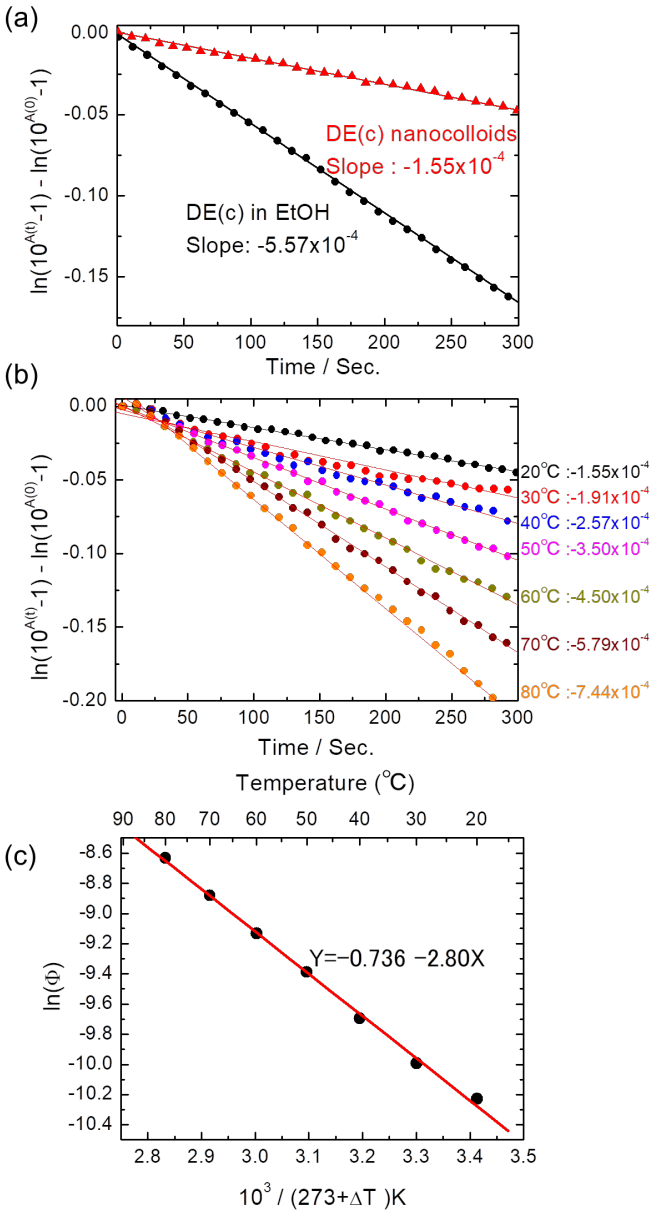

Figure S2. (a) Time profiles of the absorbance of **DE(c)-NP** and in ethanol under CW visible light irradiation (550±20 nm, 110 mW). Monitoring wavelength was set to 630 nm. Time interval of the absorption measurement was about 10 s. (b)Temperature dependence of the time profiles of the absorbance in **DE(c)-NP**. Solid lines are curves calculated with eq. S1. (c) Temperature dependence of the cycloreversion reaction quantum yield of **DE(c)-NP**.

3. Experimental setup of ns Nd: YAG laser pulse exposure

Figure S3 shows the schematic diagram of the experimental setup for single-shot ns Nd^{3+}: YAG laser pulse exposure. Light source was the second harmonic (532-nm) beam of a ns Nd^{3+}: YAG laser (Continuum, Surelight I), which repetition rate was 10 Hz and pulse duration was 6 ns fwhm. The laser power was varied by the polarizer in the range of 2 to 100 mW. After that, the beam diameter was expanded from 0.7 cm to 1.5 cm and collimated by the combination of flat concave (F = −50 cm) and flat convex (f = 100 cm) lenses. The expanded beam was focused into the sample with a cylindrical lens (f = 300). It was noted that the sample cuvette was put at the position before 100 mm from the focal point. At a sample position, the effective excitation area was estimated to be 0.27 cm^2 from the burn pattern of the laser beam (the green shaded area in the photograph in the middle of Figure S3). A sample semi-micron cuvette with an optical length of 0.4 cm was used for the ns-laser pulse exposure, indicating that the absorbance of **DE(c)-NP** was below 0.3. In this setup, the sample volume requires just 0.11 mL. These experimental conditions allow that the sample in the cuvette can be uniformly exposed by the ns laser pulse without stirring. The laser power passing through the cuvette with the rectangular window having the 0.27-cm^2 area was detected with the laser power meter (Ophir). For the absorption spectroscopy, the modular USB spectrometer (Ocean Optics, USB4000) and the identical sample semi-micron cuvette (optical length = 1.0 cm) were used (the photograph in the right of Figure S3). To cut the excitation light of the intense ns-laser pulse off, the 533-nm notch filter (Thorlabs) was inserted in front of the detector. The absorption spectra in the wavelength range of 500 to 900 nm were recorded every 1 sec during the ns-laser pulse irradiation. The kinetic data and delta absorption spectra were analysed using commercial software (Igor Pro, Wave Metrics) and homemade programs.

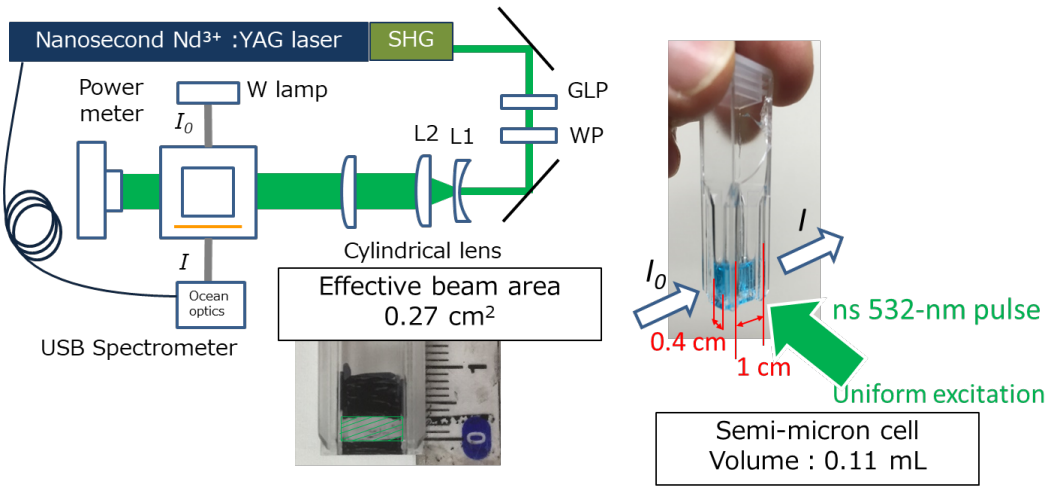

Figure S3. Experimental setup for ns Nd^{3+}: YAG laser pulse exposure. GLP: Glam laser prism, WP: wave plate, L1: Concave lens, L2: Convex lens. I_0: Intensity of incident light, I: Intensity of transmitted light.

4. Absorption spectra and size distributions of DE(c)-NP before and after ns 532-nm laser excitation

Intense ns-laser pulse exposure to the nanocolloids possibly induces the fragmentation of nanoparticles and the decomposition of **DE(c)** molecules. So, we compared the absorption spectra before and after the ns-laser pulse irradiation with the fluence of 25 mJ $cm^{-2}pulse^{-1}$ for 60 s. Figure S4(a) shows the results, together with the steady-state absorption of the **DE(o)-NP** before UV CW-light irradiation. After the laser exposure, the absorbance in the visible region due to the **DE(c)** decreased, while the band in the UV region due to the **DE(o)** increased. This indicates that the cycloreversion reaction took place without photodecomposition even by the intense ns pulse excitation. In addition, the size distributions before and after the ns laser pulse exposure were measured with the DLS technique. As a representative example, Figure S4(b) exhibited the size distribution of **DE(c)-NP** before and after the ns laser pulse exposure with the fluence of 25 mJ $cm^{-2}pulse^{-1}$ for 60 s, clearly showing the same mean diameter and distribution. This indicated that the laser fragmentation did not occur.

Integrating the above results, the laser exposure with the laser fluence of 1 to 37 mJ $cm^{-2}pulse^{-1}$ induced the cycloreversion reaction without photodecompositions and laser fragmentations.

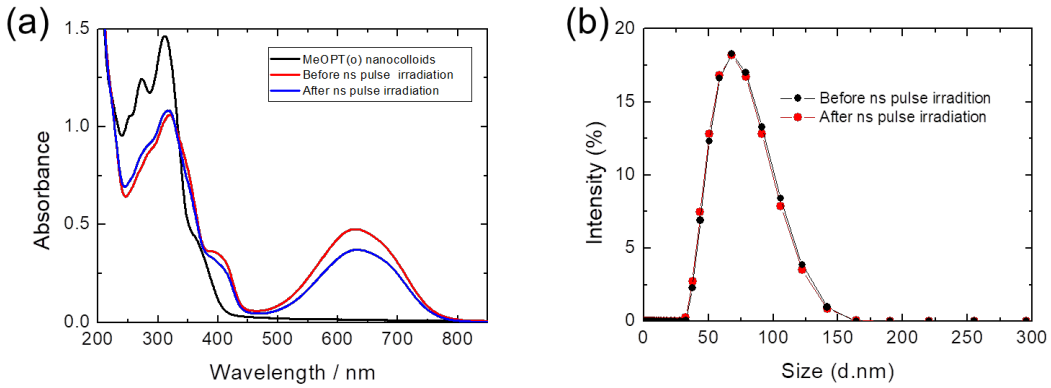

Figure S4. Absorption spectra of **DE(c)-NP** before (red) and after (blue) the ns laser pulse exposure with the fluence of 25 mJ $cm^{-2}pulse^{-1}$ for 60 s. Black line is the steady-state absorption of **DE(o)-NP** before UV CW-light irradiation. (b) Size distributions of **DE(c)-NP** before (black) and after (red) the ns laser pulse exposure obtained with the dynamic light scattering technique. The Z-average (PDI) of the **DE(c)-NP** colloids before and after the exposure was 67 nm (0.084), and 67 nm (0.076), respectively.

5. Estimation of the yield of the cycloreversion reaction by 1-shot ns pulse excitation

The procedure to estimate the conversion yield by single-shot ns pulse excitation (532 nm exc. & 6 ns fwhm) is described as follows. First, we obtained the changes in the absorbance due to the **DE(c)** as a function of the laser shot number at various laser fluences as shown in Figure S5(a). Then, the cycloreversion reaction conversion from **DE(c)** to **DE(o)** is calculated by an equation, $(A(0)-A(N)) / A(0)$, where $A(0)$ and $A(N)$ are the absorbances at 630 nm before ns laser irradiation, and after N-th shot exposure of ns pulse, respectively.

Figure S5(a) shows the results of **DE(c)-NP** at various fluences of 1, 2, 5, 7.5, 10, 15, 20, 25, 30, 37 mJ $cm^{-2}pulse^{-1}$. The conversion at any fluences increased with an increase in the laser shot number. However, the conversion at higher laser fluences showed the saturation tendency. On this saturation, we considered that it may be difficult to form a hot cluster leading to the drastic enhancement of the cycloreversion reaction because of the decrease of the ground-state **DE(c)** by the cycloreversion reaction. However, the conversion showed the linear increase to the extent of 0.1 at any fluence in Figure S5(b). The slope calculated with the linear fitting to the linear increase of the conversion against laser shot number corresponds to the conversion from **DE(c)** to **DE(o)** by the single-shot ns pulse excitation. The results of **DE(c)-NP** was shown in Figure 2a in the text.

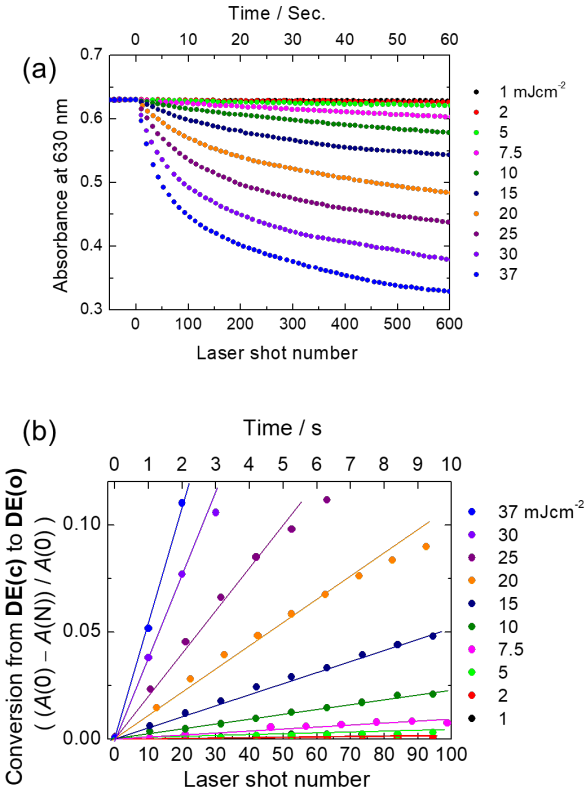

Figure S5. (a)Laser shot number dependence of the absorbance of **DE(c)-NP** at various fluences; 1, 2, 5, 7.5, 10, 15, 20, 25, 30, 37 mJ $cm^{-2}pulse^{-1}$. Monitoring wavelength was set to 630 nm. Time interval of the absorption measurement was 1 s. (b) Laser shot number dependence of the conversion of **DE(c)-NP** at various fluences. Solid lines are linear fits. The obtained slope means the conversion by single-shot pulse excitation.

Besides, we examined the laser fluence dependence of the conversion yield from **DE(c)** to **DE(o)** in the EtOH solution by using the same manner. The results are shown in Figure S5' (a) and (b).

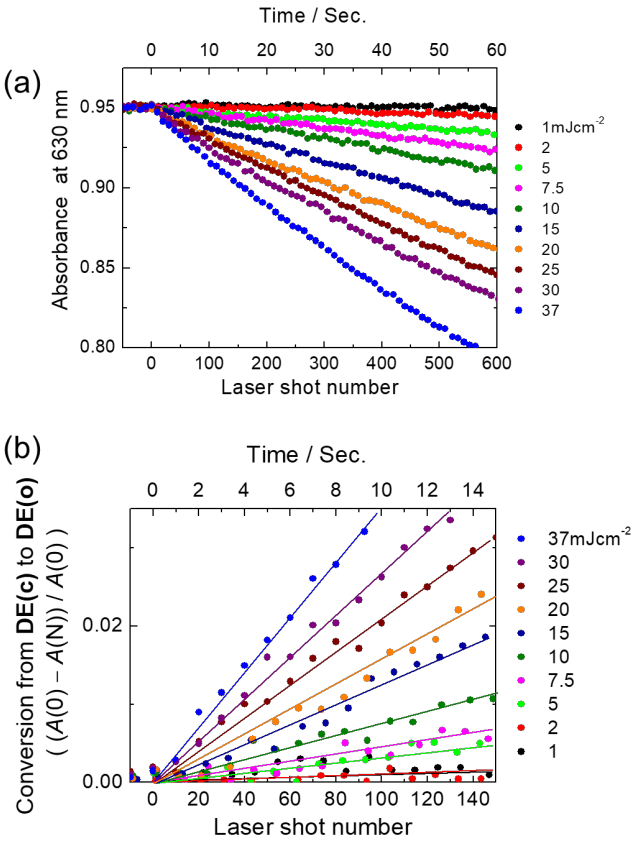

Figure S5'. (a)Laser shot number dependence of the absorbance of **DE(c)** in ethanol at various fluence; 1, 2, 5, 7.5, 10, 15, 20, 25, 30, 37 mJ $cm^{-2}pulse^{-1}$. Monitoring wavelength was set to 630 nm. Time interval of the absorption measurement was 1 s. (b) Laser shot number dependence of the conversion of **DE(c)** in the EtOH solution at various laser fluences. Solid lines are linear fits. The obtained slope means the conversion by single-shot pulse excitation.

6. Fs pump-probe spectroscopy of DE(c)-NP

Femtosecond transient absorption measurements were carried out using 100 fs pulses (800 nm) from a Ti: Sapphire chirped-pulse amplifier system operating at 1 kHz repetition rate. This beam was divided into two using a beam splitter (80% - 20%). The stronger beam was guided into an OPA system (OPA-800, Spectra-Physics) and was converted to a 540 or 560 nm pulse, which was used as a pump pulse with the intensity of 0.5 mJ pulse^{-1} at 540 nm and 25 nJ pulse^{-1} at 560 nm. The pulse duration at the sample position was estimated to be approximately 200 fs fwhm by Kerr signals of CCl_4 solution, and the focusing diameter of the pump laser was estimated to be approximately 180 μm. A small portion of the weaker fundamental beam was focused into a CaF_2 window (3-mm thickness) to generate the white-light continuum in the wavelength range of 380 to 860 nm, which was used as a probe light. The probe pulse was divided into signal and reference pulses after the white-light continuum generation, detected with a CCD camera (BU-54DUV, Bitran) coupled with a polychrometer (250is, Chromex), and sent to a personal computer for further analysis. The chirping of the monitoring white-light continuum was corrected for transient absorption spectra. The time delay between pump and probe pulses was carefully varied from −20 ps to 1800 ps by a computer-controlled translation stage (STM-150, SIGMA Koki). The home-built rotation cell (2000 rpm) with an optical length of 0.2 cm was used to avoid photodecomposition. During the measurement, we kept an initial concentration of the **DE(c)** by UV light irradiation. The room temperature was set to 20±1℃. The obtained kinetic data were analysed using commercial software (Igor 6) and homemade programs.

Figure S6(a) shows the transient absorption spectra of **DE(c)** in ethanol (2.5×10^{-4} M), excited with a fs 560-nm pulse with a laser fluence of 100 μJ cm^{-2}. Just after the excitation, the positive absorption bands around 450 and 750 nm due to the singlet excited-state absorption (ESA) and the negative band around 620 nm due to the ground-state bleaching (GSB) appeared. The ESA decreased and GSB recovered to the baseline completely in 20 ps. Figure 6(b) shows the time profiles of the transient absorbance at 750 nm and 620 nm, which can be reproduced by a single-exponential function with a time constant of 1.6 ps. That is, the excited state lifetime was 1.6 ps.

Besides, we described the explanation of the results of **DE(c)-NP**. The concentration of the **DE(c)-NP** colloids was 1.5×10^{-4} M. The excitation wavelength of 540 nm and the laser fluence of 2.5 mJ cm^{-2} were tuned. At 1 ps, the positive absorption bands around

450 and 750 nm due to the singlet ESA and the negative band around 630 nm due to the GSB appeared. The spectral shape was similar to that of the solution phase in figure S6(c). The ESA decreased and GSB recovered rapidly in 10 ps. Apart from the solution, after the decay of the S_1 state (at 50 ps), a long-lived transient species having two positive (435 and 760 nm) and two negative (630 and 700 nm) peaks remained in figure S6(c), indicating that the new transient species was generated after the decay of the singlet-excited state. After 50 ps, this new transients decayed while keeping the spectral shape. Finally, the permanent bleaching due to the cycloreversion reaction (the formation of the **DE(o)**) was slightly observed because the laser fluence was higher than that for the EtOH solution. The time profiles of the transient absorbance at 750 and 620 nm can be reproduced by a triple-exponential function. The signal at 750 nm decayed with a time constant of 1.8 ps (amplitude, 83%), grew up slightly with a time constant of 7.9 ps (12%) and decayed to the baseline with a time constant of 500 ps (5%). This behaviour was also observed at 435 nm. Here, the amplitude of the exponential function was calculated by $A_i = A_i/(\sum_{i=1}^{3} A_i)$. On the other hand, the signal at 620 nm was calculated with a triple-exponential function with three time constants of 2.0 ps (55%), 6.4 ps (15%) and 500 ps (16%), and constant value (14%). In addition, at 700 nm where the additional band (the ground-state hot band) was observed, the time profile can be reproduced with the same time constants (two decay components of 1.4 ps (98%) and 7.0 ps (20%), and a rise component of 500 ps (-18%) in figure 3(b) in the text.

Integrating above results with those of the solution, the 1.7-ps time constant was assigned to the lifetime of the singlet excited state. After the rapid relaxation of the excited state, the new transient species was formed with a time constant of 7 ps and disappeared with a time constant of 500 ps. The assignment of the new long-lived transient is detailed in Section 7.

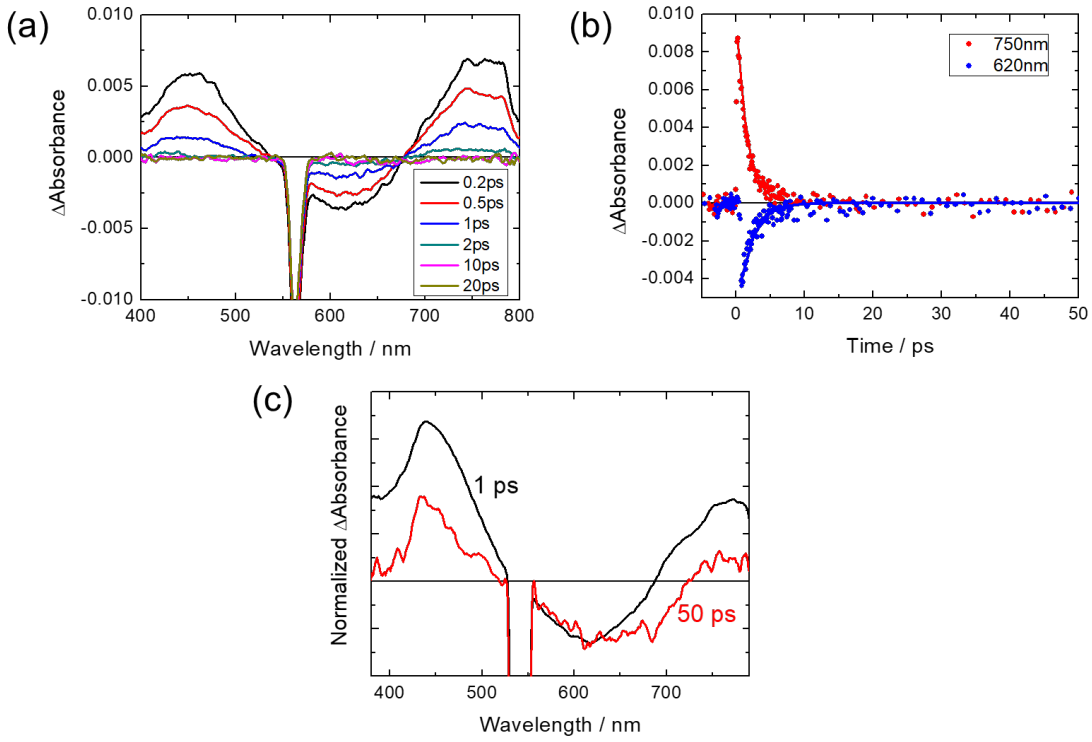

Figure S6. (a) Transient absorption spectra of **DE(c)** in ethanol, excited with a fs 560-nm pulse at 0.1 mJ $cm^{-2}pulse^{-1}$. (b) Time profiles of the transient absorbance at 620 nm (blue) and 750 nm (red). Solid lines are the calculated curve with a triple-exponential function. (c) Transient absorption spectra at 1 ps (black) and 50 ps (red), which were normalized by the transient absorbance at 610 nm. Excitation wavelength was 540 nm, and the laser fluence was at 2.5 mJ $cm^{-2}pulse^{-1}$

7. Assignment of long-lived transients of DE(c)-NP

Here, we considered the long-lived transient of **DE(c)-NP** observed by fs pump-probe spectroscopy as a hot band of the **DE(c)** ground state in the NP. Therefore, we examined the temperature dependence of the steady-state absorption spectra. An absorption spectrometer (V570, JASCO) combined with the temperature-controllable sample cell unit (TLC50F, Quantum Northwest) was used. The temperature of aqueous **DE(c)-NP** colloids was set to 20, 30, 40, and 50°C. After confirming the temperature of the colloids by a thermocouple, the absorption spectrum was measured, and then the concentration was corrected by considering the specific volume of water at each temperature. In addition, we confirmed that aggregations and decompositions were not observed at any temperature.

Figure S7(a) shows the temperature dependence of the absorption spectra of **DE(c)-NP**. With an increase in the temperature of the **DE(c)-NP** colloids, the absorbance at the peak wavelength decreased, and the spectral shape broadened. Temperature difference absorption spectra of **DE(c)-NP** were obtained by subtracting the reference absorption spectrum at 20°C from the absorption spectra at different temperatures (30, 40, and 50°C). Figure S7(b) shows the results, together with the transient absorption spectrum at 50 ps. For example, at 30°C, two positive bands around 435 and 750 nm and negative band with two peaks at 630 and 690 nm appeared, which is indicative of the hot band of the **DE(c)** ground state in the NP at +10°C. With an increase in the temperature, the intensity of delta absorbance increased while the spectral shape keeping. The spectral shape of the transient absorption spectrum at 50 ps after the excitation, which corresponded to the long-lived transient species, was similar to that of the temperature difference spectra. This indicates that the long-lived transient can be safely assigned to the hot band of the ground state of the **DE(c)**. In contrast, we concluded that the triplet state of the **DE(c)** was not formed in the nanocollouds. Moreover, to estimate the transient temperature via photothermal energy conversion by the *femtosecond pump pulse*, the standard curve was developed based on the ratio of the temperature difference absorbance at 690 nm and 750 nm as shown in Figure 7(c). The ratio calculated from the transient absorption spectrum at 50 ps was 0.56. As a result, at the laser fluence of 2.5 mJ cm^{-2}, the transient temperature of the **DE(c)-NP** was roughly estimated to be +23K. This indicated that the **DE(c)-NP** is elevated transiently after the rapid internal conversion in a few ps time scale.

Integrating the above results with fs-TA data in section 6, the cycloreversion reaction

and the subsequent process are summarized in Figure S7(d). After rapid decay of the singlet excited state with a time constant of 1.7 ps, "hot" nanoparticles were formed with a time constant of 7 ps. That is, the rapid non-radiative decay of the excited state led to the increase of the transient temperature of the nanoparticles. Because "hot" nanoparticles were surrounded by water, they were cooled down with a time constant of 500 ps.

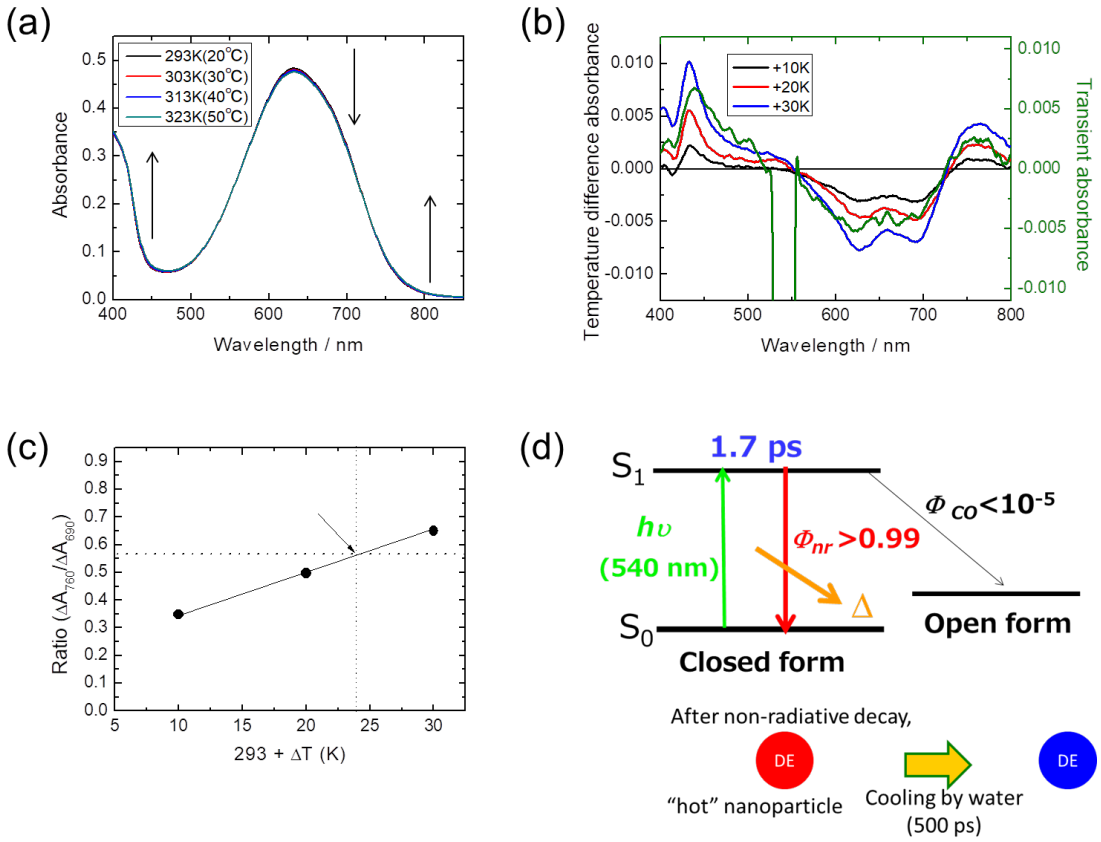

Figure S7. (a) Dependence of absorption spectra of aqueous **DE(c)-NPs** colloids on the temperature of 20, 30, 40 and 50°C. (b) Temperature difference spectra of aqueous **DE(c)-NPs** colloids obtained by subtracting the reference absorption spectrum at 20°C from the absorption spectra at different temperatures. Green line is the transient absorption spectrum at 50 ps. (c) Standard curve of the transient temperature based on the temperature difference absorption spectra. An arrow is the ratio of the transient absorption spectra at 50 ps. (d) Schematic illustration of the cycloreversion reaction and the subsequent processes of **DE(c)-NP**.

8. Estimation of the density of excited molecules by ns laser pulse excitation

Here, we describe how to estimate the density of excited molecules at unit time in the 6-ns laser pulse.

Under weak excitation condition, photophysical processes of **DE(c)** are as follows.

Absorption:	$S + h\nu_i \rightarrow S^*$
Fluorescence deactivation:	$S^* \rightarrow S + h\nu_f$
Internal conversion:	$S^* \rightarrow S$
Intersystem crossing:	$S^* \rightarrow T^*$
Photoinduced reaction :	$S^* \rightarrow O$

S and S* are the singlet ground state of the **DE(c)**, S* is the singlet excited state of the **DE(c)**, T* is the triplet excited state of the **DE(c)**, and O is the ground state of the **DE(o)**. $h\nu_i$ and $h\nu_f$ are the energies of the excitation and fluorescence photons, respectively. The rate equation for S* usually can be written by eq. S3.

$$\frac{d[S^*]}{dt} = \sigma I[S] - (k_{ic} + k_f + k_{isc} + k_r)[S^*] \quad \text{(eq. S3)}$$

Here, σ is the absorption cross-section of the **DE(c)** at excitation wavelength [cm^2 $molecule^{-1}$], and I the photon flux density of the excitation light with the dimension of the number of photon divided by unit area size and the time [photon cm^{-2} s^{-1}]. k_{ic} is the rate constant of the internal conversion [s^{-1}], k_f the rate constant of the fluorescence deactivation [s^{-1}], k_{isc} the rate constant of the intersystem crossing to the triplet state [s^{-1}], and k_r the rate constant of the cycloreversion reaction [s^{-1}]. [S^*] and [S] are the concentrations of S* and S, respectively. By using these rate constants, the excited-state lifetime of the **DE(c),** τ [s] is expressed as $\tau = 1/(k_{ic} + k_f + k_{isc} + k_r)$.

k_{isc} is close to zero because the triplet excited state was not detected by the fs transient absorption spectroscopy in section 6. **DE(c)** has quite low quantum yields of the cycloreversion reaction and emission (fluorescence) so that k_{ic} is much larger than k_f and k_r. These results mean $k_{ic} \approx k_{ic} + k_f + k_{isc} + k_r$, and $\tau = 1/k_{ic}$. In addition, by considering that the total concentration of the **DE(c)** , $[S]_0$ is the sum of [S] and [S^*] ($[S]_0$ = [S] + [S^*]), Eq. S3 is re-expressed by eq. S4.

$$\frac{d[S^*]}{dt} = \sigma I[S]_0 - (\sigma I + k_{ic})[S^*] \quad \text{(eq. S4)}$$

Here, we consider the value of $\sigma \times I$ corresponding to the transition probability. Since the unit of I is expressed by photon cm^{-2} s^{-1}, the dimension of $\sigma \times I$ is s^{-1}. First, the σ of **DE(c)** at 532 nm was calculated from molar absorption coefficient, ε_c^{NP} and the molecular density of **DE(c)** in **DE(c)-NP**, $\rho_{DE(c)}$. Using the values of ε_c^{NP} = 4400 $M^{-1}cm^{-1}$ and $\rho_{DE(c)}$ = 2.0 M, σ was estimated to be 1.7×10^{-17} cm^2 $molecule^{-1}$. Next, we consider the value of I. For the calculation, the temporal profile of the laser pulse is assumed to be a square wave, and the width is set to the pulse duration (6-ns fwhm). The value of I was calculated by the following equation, $I = laser\ fluence\ [Jcm^{-2}]/(photon\ energy\ [J] \times pulse\ duration\ [s])$. For example, when the laser fluence of the ns-laser pulse (excitation wavelength: 532 nm, pulse duration: 6 ns) is 37 mJ $cm^{-2}pulse^{-1}$, which is the maximum value of our laser experimental condition, I was estimated to be 1.7×10^{25} photon $cm^{-2}s^{-1}$. The value of $\sigma \times I$ is calculated to be 2.9×10^8 s^{-1}. On the other hand, k_{ic} was 5.8×10^{11} s^{-1}, which was the inverse of the excited state lifetime of **DE(c)** (1.7 ps) from the fs transient absorption data in figure 3 and figure S6. The value of k_{ic} is much larger than that of the transition probability ($\sigma \times I$). This means that [S*] keeps much lower as compared to [S] during the ns-laser pulse irradiation. Eq. S4 is approximated by eq. S5.

$$\frac{d[S^*]}{dt} = \sigma I[S]_0 - k_{ic}[S^*] \qquad \text{(eq. S5)}$$

The solution of this differential equation ([S*(0)] = 0 at t = 0) is finally given by eq. S6.

$$\frac{[S^*(t)]}{[S]_0} = \frac{\sigma I}{k_{ic}}(1 - e^{-k_{ic}t}) \qquad \text{(eq. S6)}$$

At the laser fluence of 37 mJ $cm^{-2}pulse^{-1}$, the concentration ratio of [S*(t)] to $[S]_0$ is calculated to be ca. 4.9×10^{-4}. Since the value of the ratio is very small, the percentage that the excited-state **DE(c)** molecules are neighbouring each other is negligibly low. From this calculation, we can safely conclude that the cooperative photochemical reaction model is ruled out.

Besides, we consider the possibility of the stepwise two-photon absorption of a molecule such as S + hν → S* + hν → product (S and S* are the same molecule) under ns-laser pulse excitation. Here, we evaluate the time interval between photons (photon interval) in ns-laser pulse by using $\sigma \times I$ in eq. S5. The inverse of $\sigma \times I$ corresponds to the photon interval, and the dimension is s. If the photon interval is shorter than the excited-state lifetime, the molecule excited by the first one photon can interact with the second

one photon during a laser pulse. In the present experiments by using ns-laser pulse, for example, $1/(\sigma \times I)$ is calculated to be 3.4 ns for 37 mJ $cm^{-2}pulse^{-1}$, 6.5 ns for 20 mJ $cm^{-2}pulse^{-1}$, and 13 ns for 10 mJ $cm^{-2}pulse^{-1}$. These values were much longer than the S_1 state lifetime of 1.7 ps for the **DE(c)-NP** or 1.6 ps for the EtOH solution, indicating that the molecule excited by the first one photon cannot absorb the second one photon in the 6-ns laser pulse. If a ps-laser pulse (532 nm, 15 ps fwhm, 37 mJ $cm^{-2}pulse^{-1}$) is applied to the excitation of the **DE(c)**, the photon interval is 8.5 ps, which is close to the S_1-state lifetime. In this case, the stepwise two-photon absorption will be possibly induced by the ps-laser pulse. In relation to this, Miyasaka et al has already demonstrated that the 532-nm ps-laser pulse excitation enhanced the cycloreversion reaction of several diarylethene derivatives in solution phase, which mechanism was explained as the stepwise two-photon absorption via the S_1 state ($S + h\nu \rightarrow S^* + h\nu \rightarrow S_n \rightarrow$ open form).[5-7] In this case, the reaction yield of the higher excited (S_n) state was larger than that of the S* state. Also, they reported that ns-laser pulse did not induce the stepwise two-photon absorption at the laser fluence of <1 mJ $cm^{-2}pulse^{-1}$. Integrating above results and discussion, we can safely conclude that the stepwise two-photon absorption via "the S_1-state molecule" is ignored in the **DE(c)-NP** and the EtOH solution.

Instead, in the **DE(c)-NP**, the vibrationally-excited molecule after the rapid internal conversion was observed in Figure S6. This molecule is a candidate for the absorber of the second photon because of the longer lifetime as compared to the S_1 state. However, the lifetime of 0.5 ns is shorter than the above photon intervals. This means that one vibrationally-excited molecule also cannot absorb the second photon. However, since one excited molecule is surrounded by ground-state molecules in the NP, the heat generated via the rapid internal conversion of the excited molecule is diffused into the neighbouring ground-state molecules, and a cluster consisting of plural vibrationally-excited molecules (e.g. 10-20 molecules) is formed in a few ps time scale and survives in a few tens to a hundred of ps time scale [8-13] as shown in Scheme 2 in the text. This means that the value of σ apparently and temporally increases up to 10-20 $\times \sigma$. In this case, the photon interval (0.34 - 0.17 ns at 37 mJ $cm^{-2}pulse^{-1}$) is close to the lifetime of the vibrationally-excited molecule (0.5 ns). As a result, the vibrationally-excited molecules may absorb the second photons. That is, the increase of the number of the vibrationally-excited molecule allows the stepwise two-photon absorption even under ns-laser pulse excitation. It is notable that, in our proposed stepwise two-photon absorption, a molecule excited by the first one

photon is different from a molecule absorbing the second one photon. We consider when another photon is absorbed by any molecules in the hot cluster, the enhanced cycloreversion reaction may take place. In other words, the formation of the hot cluster plays an important role in the enhancement of the cycloreversion reaction under ns-laser pulse excitation.

9. Numerical simulation of the transient temperature of DE(c)-NP

First, we consider the maximum transient temperature (ΔT_{max}) in the text. Given that all the energy of excitation light absorbed by a particle converts into heat, the relation between the transient temperature elevation (ΔT [K]) and the excitation energy (E [J]) is expressed by the following equation.

$$\Delta T_{max} = \frac{E}{C_p \times m \times \rho \times V} \qquad \text{(eq. S7)}$$

Here, C_p is the specific heat capacity [J g^{-1} K^{-1}], m is the molecular weight [g mol^{-1}], ρ is the molecular density [mol cm^{-3}], and V is the volume [cm^3] of the nanoparticle.

The excitation energy absorbed by the nanoparticle is presented by eq. S8.

$$E = F \times (1 - 10^{-A}) \times S_P \qquad \text{(eq. S8)}$$

Here, F, is the laser fluence [J cm^{-2}], A is the absorbance at the excitation wavelength, and, S_P is the absorption cross-section of the particle [cm^2]. Because the absorbance of one nanoparticle is much less than 0.1, eq. S8 is approximated by eq. S9.

$$E = F \times A \times S_P \qquad \text{(eq. S9)}$$

For simple calculation, given that the shape of nanoparticles is considered to be the cube with r [cm] on a side and A equals to $\varepsilon \times \rho \times r$ from Lambert-Beer's low, the substitution of eq. S9 in eq. S7 leads to eq. S10. Here, ε is the absorption coefficient [$M^{-1}cm^{-1}$].

$$\Delta T_{max} = \frac{\varepsilon \times F}{C_p \times m} \qquad \text{(eq. S10)}$$

In this study, ε was replaced with the molar absorption coefficient of the **DE(c)-NP**, ε_c^{NP} at 532 nm (4400 $M^{-1}cm^{-1}$). Parameter values for our experimental condition are m= 552.55 g mol^{-1} and C_p= 1.1 J $g^{-1}K^{-1}$.[14] For example, when the F is 20 mJ $cm^{-2}pulse^{-1}$, ΔT_{max} is calculated to be 140K.

Next, we consider changes in the transient temperature of the **DE(c)-NP** by single ns-pulse laser excitation. Our model starts with the energy balance equation (eq. S11) where energy is supplied by the absorption of one **DE(c)-NP** in water by ns pulse laser light (Q_{in}) and dissipated by transfer to the surrounding water (Q_{out}).[15-18] It is noted that the simulated temperature corresponds to an average temperature over the excited **DE(c)-NP**. The time-dependent temperature change in thermal energy of the **DE(c)-NP** is determined by the rate of heat input from the laser ($Q_{in}(t)$) through the nanoparticles and the rate of heat dissipation to the external environment ($Q_{out}(t)$) and it expressed by the following equation.

$$mC_p \frac{dT^{NP}(t)}{dt} = Q_{in}(t) - Q_{out}(t) \quad \text{(eq. S11)}$$

T^{NP} is the temperature of the NP, and t is the delay time. The rate of heat input through the nonradiative deactivation of excited **DE(c)** molecules in nanoparticles by ns-pulse excitation ($Q_{in}(t)$) was expressed by eq. S12, where k_{th} is the rate of the thermalization of the NP and η is the light-to-heat conversion efficiency. $I(t)$ is the time-dependent pulse function with photon density.

$$Q_{in}(t) = k_{th} \times I(t) \times \varepsilon \times \eta \quad \text{(eq. S12)}$$

The rate of energy flowing out of the system, which equals to the cooling by water ($Q_{out}(t)$) was presented by eq. S13.

$$Q_{out} = h \times S \times [T^{NP}(t) - T(0)] \quad \text{(eq. S13)}$$

Here, h is a heat transfer coefficient. $T(0)$ is the ambient room temperature of the surrounding water and assumed to be constant and 293K. The dissipation energy is assumed to be proportional to a linear thermal driving force. Eq. S11 can be described as a simple form (eq. S14) by collecting terms and transient temperature, $\Delta T = T^{NP}(t) - 293$.

$$\frac{d\Delta T(t)}{dt} = \frac{\varepsilon \times I(t)}{C_p \times m} \times \eta \times k_{th} - \frac{h \times S}{C_p \times m} \Delta T(t) \quad \text{(eq. S14)}$$

Here, we defined $k_{th} \equiv k_n$, and η was set to be 1 because the quantum yield of the nonradiative relaxation of the excited state is close to 1. In the same way, $\alpha \equiv \frac{h \times S}{C_p \times m}$ was defined as the rate constant of the heat dissipation from **DE(c)-NP** to surrounding water (cooling rate). k_n is the inverse of the S_1-state lifetime and α can be determined by measuring the time profile of the "hot band" of the ground state in the nanoparticles in Figure S6. On the other hand, $I(t)$ is defined as a normalized Gaussian function of by taking the ns pulse duration (ω) and laser power (fluence, F) into account, and it is given by eq. S15. $u(t)$ is the normalized Gaussian function.

$$I(t) = \frac{F}{\sqrt{2\pi\omega^2}} \exp\left(-\frac{t^2}{2\omega^2}\right) = F \times u(t) \quad \text{(eq. S15)}$$

By inserting eq. S15 into eq. S14, we obtain the following equation.

$$\frac{d\Delta T}{dt} = \Delta T_{max} \times u(t) \times k_n - \alpha \times \Delta T \quad \text{(eq. S16)}$$

Based on the eq. S16, we finally obtained the following equation as the time profile of the temperature of the **NP**.[18]

$$T^{NP}(t) = 293 + \Delta T = 293 + \Delta T_{max}\{[1 - \exp(-k_n t)] \exp(-\alpha t) \otimes u(t) \quad \text{(eq. S17)}$$

The term of $[1-\exp(-k_n t)]$ describes the build-up of the transient temperature of the NP through the nonradiative deactivation of excited molecules.

The numerical simulation by using eq. S17 was carried out and the results are shown in Figure S8. Parameter values for our experimental condition were k_n = 1.7 ps^{-1}, α = 500 ps^{-1}, m = 552.55 g mol^{-1}, C_p = 1.1 J g^{-1}mol^{-1},[14] and ε (ε_C^{NP}) = 4.4×10^3 M^{-1}cm^{-1}. F is applied to experimental laser fluences.

First, the fs pulse (ω = 200 fs) was applied to the simulation in Figure S8(a). In this simulation, the laser fluence was set to 2.5 mJ cm^{-2}pulse^{-1}, which was the same value in fs-TAS measurement. The very quick elevation of T^{NP} was followed by the depression with a time constant of 500 ps. The maximum value of the transient temperature profile (T_{max}^{NP}) was obtained to be 293+20K. The transient temperature of +20K was consistent with the value calculated by eq. S10. This indicated that because the temperature elevation and cooling times were much longer than the fs pulse duration, the temperature of the NP could attains the maximum value of 293+20K. In addition, the value of T_{max}^{NP} agreed with the obtained one from the fs-TAS data in Figure S7 and Figure 3 in the text. These results means that the numerical simulation model is appropriate for the estimation of the value of T_{max}^{NP}.

Next, the ns pulse (ω = 6 ns) was applied to the simulation. Figure S8(b) showed the representative result at the laser fluence of 20 mJ cm^{-2}pulse^{-1}. Without the cooling, the transient temperature increased with the response function of the 6-ns pulse, and attained to the value of T_{max}^{NP}=293+140K in 10 ns. On the other hand, with the cooling process, the elevation and depression of the transient temperature finished in 10 ns. The T_{max}^{NP} was just 9.1K. Considering that the lifetime of the S_1-state (the inverse of the rate of the thermalization, $1/k_n$ = 1.7 ps) and the lifetime of the hot band (the inverse of the rate of the cooling, 1/α = 500 ps) are shorter than the ns pulse duration, the cooling has started before the temperature of the NP completely rises up to 293+140K. Therefore, the T_{max}^{NP} drastically decreased in the ns pulse. However, the duration time that the NP keeps the temperature high by a 6-ns pulse excitation lasted longer than that by a 200-fs pulse. This duration time will also play an important role in the excitation of **DE(c)** molecules in "hot" **DE(c)-NP**.

The other results at different laser fluences are shown in Figure 8(c). At any laser fluences, the transient temperature went up to maximum value and dropped to zero in 10

ns. The values of T_{max}^{NP} at any fluences also drastically decreased those estimated with eq. S10. For Figure 4(b) in the text, we obtained the maximum transient temperature at each laser fluence from Figure S8(a) and plotted it as a function of the laser fluence.

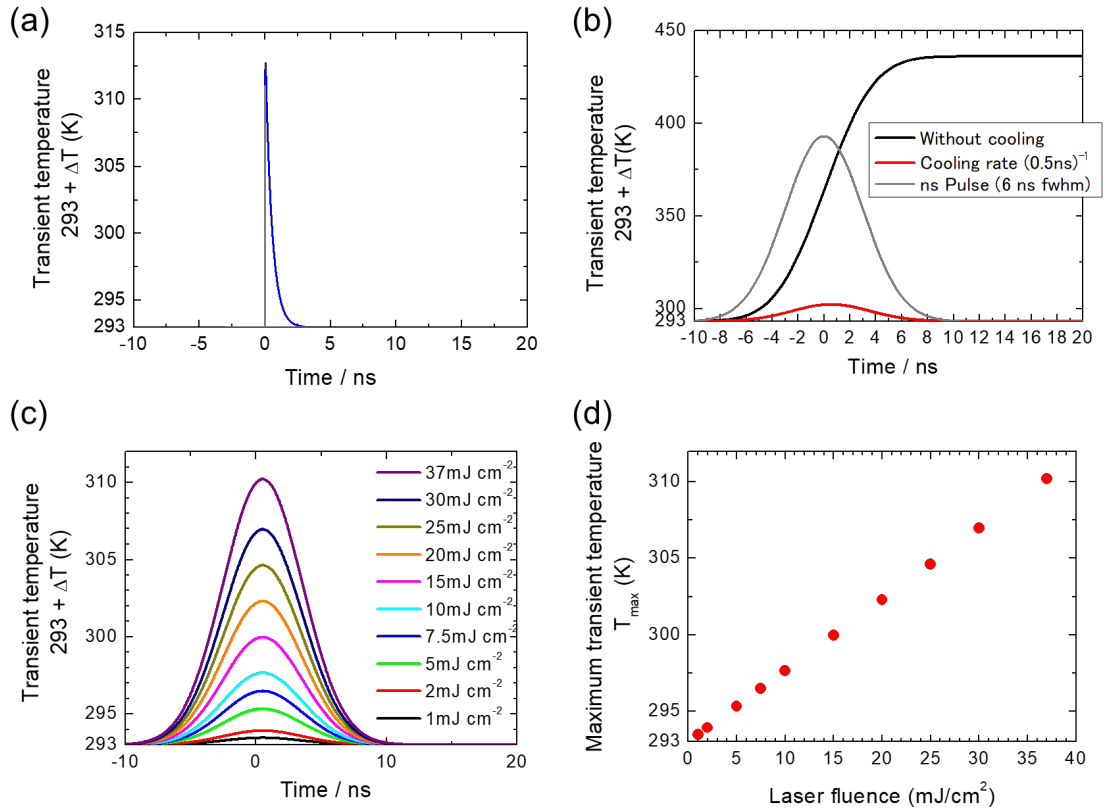

Figure S8. (a) and (b) Simulated time evolutions of the transient temperature of **DE(c)-NP** in water (a) by a fs pulse excitation and (b) by a ns pulse excitation. The fs pulse duration was 200 fs, and the laser fluence was 2.5 mJ $cm^{-2}pulse^{-1}$. The ns pulse duration was 6 ns, and the laser fluence was 20 mJ $cm^{-2}pulse^{-1}$. (c) Dependence of the transient temperature on the laser fluence at 1, 2, 5, 7.5, 10, 15, 20, 25, 30, and 37 mJ $cm^{-2}pulse^{-1}$. (b) Relationship between the laser fluence and the maximum transient temperature, T^{NP}_{max} calculated by eq. (3) in the text.

10. References:

1. K. Morimitsu, K. Shibata, S. Kobatake and M. Irie, *J. Org. Chem.*, 2002, **67**, 4574-4578.
2. H. Kasai, H. Oikawa, S. Okada and H. Nakanishi, *Bull. Chem. Soc. Jpn.*, 1998, **71**, 2597-2601.
3. N. Tagawa, A. Masuhara, H. Kasai, H. Nakanishi, and H. Oikawa, *Mol. Cryst. Liq. Cryst.*, 2010, **520**, 245-250.
4. Y. Ishibashi, T. Umesato, S. Kobatake, M. Irie, and H. Miyasaka, *J. Phys. Chem. C,* 2012, **116**, 4862-4859.
5. Y. Ishibashi, K. Okuno, C. Ota, T. Umesato, T. Katayama, M. Murakami, S. Kobatake, M. Irie and H. Miyasaka, *Photochem. Photobiol. Sci.*, 2010, **9**, 172-180.
6. M. Murakami, H. Miyasaka, T. Okada, S. Kobatake, M. Irie, *J. Am. Chem. Soc.*, 2004, **126**, 14764-14772.
7. H. Sotome, T. Nagasaka, K. Une, S. Morikawa, T. Katayama, S. Kobatake, M. Irie and H. Miyasaka, *J. Am. Chem. Soc.*, 2017, **139**, 17159-17167.
8. V. Balevicius, Jr., T. Wei, D. Di Tommaso, D. Abramavicius, J. Hauer, T. Polivka and C. D. P. Duffy, *Chem. Sci.*, 2019, **10**, 4792-4804.
9. H. Kim and D. D. Dlott, *J. Chem. Phys.*, 1991, **94**, 8203-8209.
10. S. Chen, I.-Y. S. Lee, W. A. Tolbert, X. Wen and D. D. Dlott, *J. Phys. Chem.*, 1992, **96**, 7178-7186.
11. X. Wen, W. A. Tolbert and D. D. Dlott, *Chem. Phys. Lett.*, 1992, **192**, 315-320.
12. X. Wen, W. A. Tolbert and D. D. Dlott, *J. Chem. Phys.*, 1993, **99**, 4140-4151.
13. A. Tokmakoff, M. D. Fayer, and D. D. Dlott, *J. Phys. Chem.* 1993, **97**, 1901-1913.
14. M. V. Roux, M. Temprado, J. S. Chickos, and Y. Nagano, *J. Phys. Chem. Ref. Data*, 2008, **37**, 1855-1996.
15. K. Jiang, D. A. Smith and A. Pinchuk, *J. Phys. Chem. C*, 2013, **117**, 27073-27080.
16. H. H. Richardson, M. T. Carlson, P. J. Tandler, P. Hernandez and A. O. Govorov, *Nano Lett.*, 2009, **9**, 1139-1146.
17. V. K. Pustovalov, *Chem. Phys.*, 2005, **308**, 103-108.
18. C. K. Sun, F. Vallée, L. Acioli, E. P. Ippen, and J. G. Fujimoto, *Phys. Rev. B*, 1993, **48**, 12365-12368.